

Electron-Induced Dissociation of CO₂ on TiO₂(110)

Junseok Lee,^{*,†,‡} Dan C. Sorescu,[†] and Xingyi Deng^{†,‡}

[†]National Energy Technology Laboratory, Department of Energy, Pittsburgh, Pennsylvania 15236, United States

[‡]URS, P.O. Box 618, South Park, Pennsylvania 15129, United States

S Supporting Information

ABSTRACT: The electron-induced dissociation of CO₂ adsorbed at the oxygen vacancy defect on the TiO₂(110) surface has been investigated at the single-molecular level using scanning tunneling microscopy (STM). Electron injection from the STM tip into the adsorbed CO₂ induces the dissociation of CO₂. The oxygen vacancy defect is found to be healed by the oxygen atom released during the dissociation process. Statistical analysis shows that the dissociation of CO₂ is one-electron process. The bias-dependent dissociation yield reveals that the threshold energy for electron-induced dissociation of CO₂ is 1.4 eV above the conduction-band minimum of TiO₂. The formation of a transient negative ion by the injected electron is considered to be the key process in CO₂ dissociation.

Activation of CO₂ followed by its chemical conversion into useful organic compounds can be a key process in reducing the amount of CO₂ emitted by human activity and potentially utilizing (or reusing) the CO₂ to generate useful products.¹ The thermal reduction of CO₂ requires high temperatures because of the thermodynamic stability of the CO₂ molecule.² One of the promising alternatives is the reduction of CO₂ using photogenerated electrons on photocatalysts.³ Electron-transfer processes on photocatalysts such as TiO₂ are thus a primary area of research in the photoreduction of CO₂.⁴ Since the discovery of the photoactivity of TiO₂,^{5,6} considerable progress in understanding various chemical and physical processes on TiO₂ surfaces has been made.⁷ The photoreduction of CO₂ is a multistep process involving both activation of CO₂ and dissociation of the OC–O bond. The key initial step is the activation of CO₂ through the transfer of photogenerated electrons in the photocatalyst.⁸ Despite the wide use of TiO₂ in photocatalysis,⁹ especially in CO₂ photoreduction studies,³ to the best of our knowledge, little atomic-scale understanding of electron-induced chemistry of CO₂ on the TiO₂ surface is available. In this work, we used tunneling electrons from the STM tip^{10–13} to induce dissociation of individual CO₂ molecules adsorbed at oxygen vacancy defects on a model photocatalyst TiO₂(110) surface, aiming to provide a microscopic view of the electron-induced CO₂ activation process. The oxygen vacancy defect has been found to be healed by the O atom released during the dissociation of CO₂. We further demonstrate that the dissociation of CO₂ is driven by a one-electron process with a threshold energy of 1.4 eV above the conduction-band minimum (CBM) of TiO₂.

A schematic of the TiO₂(110) surface containing an oxygen vacancy defect (V_O),¹⁴ a bridging hydroxyl (OH_b),¹⁵ and a CO₂ adsorbed at a V_O site¹⁶ is shown in Figure 1A along with an inset figure depicting the tilted adsorption geometry of CO₂ at the V_O site.¹⁶ The most stable adsorption of CO₂ on TiO₂(110) takes place at the V_O site in a nearly linear configuration with an adsorption energy of 0.44 eV. One of the oxygen atoms of the CO₂ is located slightly above the plane of the bridging oxygen (O_{br}) rows while the molecular axis of CO₂ is tilted away from the surface normal by 57° along the [110] direction.¹⁶

An STM image of the TiO₂(110) surface after exposure to CO₂ at 55 K is shown in Figure 1B. Virtually all the V_O sites are occupied with the CO₂ features (marked with diamonds), which are brighter than the OH_b features (circles). The inset STM images in Figure 1B show the same area of the surface before and after thermal diffusion of two CO₂ molecules away from their V_O sites (dotted ellipses), clearly revealing the V_O sites under CO₂. This is in agreement with the results of previous thermal desorption studies.^{17,18} To compare the apparent heights, we show in Figure 1C a high-resolution STM image wherein V_O, OH_b, and CO₂ features are found in close proximity. The CO₂ feature is the brightest among the three. Height profiles along the lines over the CO₂ (red) and OH_b (green) are shown in Figure 1D. The apparent height of the CO₂ feature is 80 pm with respect to the Ti row. The symmetrical height profile of the CO₂ feature does not represent the theoretical adsorption configuration shown in Figure 1A, probably because of the rapid thermal motion of CO₂ at V_O at 55 K.¹⁹

Dissociation of an adsorbed CO₂ molecule occurs when a positive voltage pulse is applied to the molecule. Figure 2A shows an STM image of a surface area where most of the V_O sites are occupied by CO₂ molecules. Positive voltage pulses (+2.0 V, 5 pA, 1 s) were applied to each marked CO₂ feature during the scan in the upward direction (Figure 2B). Sharp discontinuities of the CO₂ features were observed immediately after the voltage pulses. The following scan of the same area (Figure 2C) revealed dark O_{br} rows without any CO₂ or V_O features at the marked positions. This suggests that the V_O sites were healed by O atoms released from the CO₂ molecules upon dissociation of the C–O bond. It seems that of the two C–O bonds in the CO₂, only the one involving the V_O-bound O dissociated, as the dissociation of CO₂ always healed V_O. We did not observe any adsorbed CO or O fragments that would otherwise be found on Ti rows.²⁰ We also note that the dissociation of CO₂ by voltage pulses is a local process, as voltage pulses to a CO₂ feature did not affect the adjacent CO₂ molecules.

Received: May 3, 2011

Published: June 07, 2011

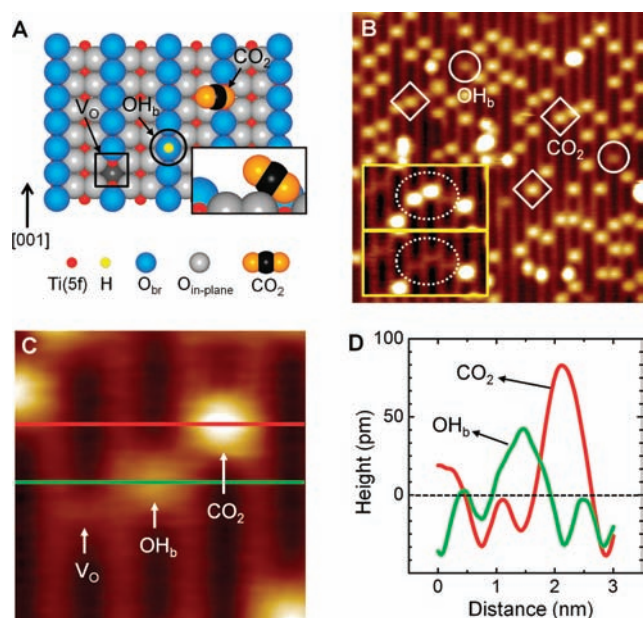


Figure 1. (A) Schematic showing an oxygen vacancy defect (V_O) (black square), a bridging hydroxyl (OH_b) (black circle), and a CO_2 molecule adsorbed at a V_O site on the reduced $TiO_2(110)-(1 \times 1)$ surface. Fivefold-coordinated $Ti(5f)$ atoms and bridging oxygens (O_{br}) are indicated in red and blue respectively. The molecular axis of the adsorbed CO_2 is perpendicular to the direction of the bridging-oxygen row ($[001]$ azimuth) and is tilted away from the surface normal by 57° , as shown in the inset figure. (B) STM image (1.5 V, 5 pA, 15 nm \times 15 nm) of the $TiO_2(110)$ surface after adsorption of CO_2 at 55 K. All of the V_O sites are occupied by CO_2 . Three CO_2 and two OH_b features are marked with diamonds and circles, respectively. The inset shows two STM images (5.1 nm \times 2.6 nm) of the same area on the surface. Two CO_2 molecules (in the dotted ellipse in the upper inset) diffused away from their V_O sites, leaving two intact V_O sites visible (lower inset image). (C) STM image (1.5 V, 5 pA, 3 nm \times 3 nm) of an area where three different features (CO_2 , OH_b , and V_O) are shown for comparison. (D) Height profiles along the red (over CO_2) and green (over OH_b) lines in C. The apparent height of the Ti rows is set to zero (dashed line).

In our work, electron injection into CO_2 was essential for dissociation of the molecule. Voltage pulses with negative biases in the range from -1.5 to -2.5 V did not result in any dissociation events out of 65 tries, suggesting that injection of holes cannot induce the dissociation of CO_2 . Electric-field-induced dissociation of CO_2 was unlikely because the electric field calculated in our experiments was always less than 2.53 V/nm, far below the minimum value of 40 V/nm required to dissociate a CO_2 molecule²¹ [see Figure S1 in the Supporting Information (SI)]. Thermal dissociation of CO_2 was also ruled out because of the high thermal activation energy needed to dissociate the C–O bond (the dissociation energy of the C–O bond in neutral CO_2 is 5.45 eV in the gas phase²²). We show in Figure S2 that hypothetical thermal dissociation of CO_2 at V_O on $TiO_2(110)$ leading to either adsorbed or desorbed CO requires at least 1.69 eV of thermal activation energy. However, it is likely that the CO_2 molecule would desorb from $TiO_2(110)$ before the thermal dissociation could take place, in view of the fact that the adsorption energy of CO_2 at V_O on $TiO_2(110)$ is 0.44 eV.¹⁶ Moreover, one would expect to observe nonlocal dissociation/desorption events in the thermal process. We therefore conclude that the dissociation of CO_2 observed in this work is an *electron-induced* process.

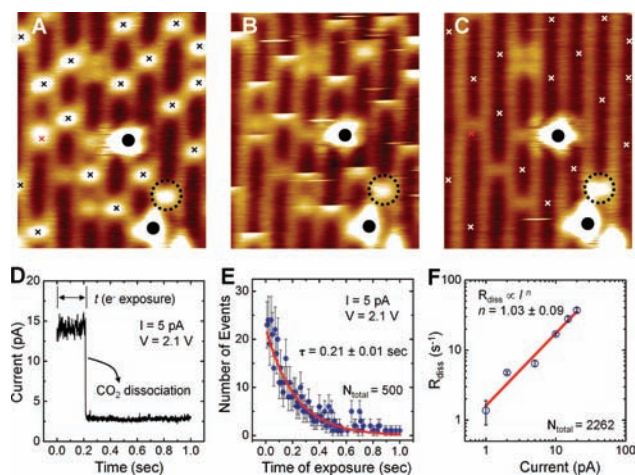


Figure 2. (A) STM image (1.5 V, 5 pA, 5.1 nm \times 6.4 nm) of the $TiO_2(110)$ surface before voltage pulses were applied to 18 adsorbed CO_2 features (marked with \times symbols). Two unknown bright features (marked with black dots) were used as reference positions. The feature with a red \times is a CO_2 feature located right next to an unknown adsorbate. (B) During the upward scan of the area, voltage pulses ($+2.0$ V, 5 pA, 1 s) were applied to each CO_2 feature marked in A. Because of dissociation, only the lower portions of the CO_2 features are visible. Adjacent CO_2 molecules were not affected by the voltage pulses. For comparison, no voltage pulse was applied to the CO_2 in the dotted circle. Some sharp noise lines appear, probably caused by the unstable tip condition after pulsing or mobile fragments. (C) STM image of the same area after application of the voltage pulses. White \times symbols represent the original positions of the adsorbed CO_2 molecules before the voltage pulses. Dark O_{br} rows resulting from healing of the V_O sites are clearly visible. The CO_2 feature in the dotted circle remained intact. In the lower-left part of the image, four V_O features are visible that can be associated with brighter features at the corresponding positions in A. A slight change in the shape of the reference object was observed after the pulsing experiment. (D) Tunneling current trace during a $V = +2.1$ V, $I = 5$ pA pulse. Electrons tunneled from the STM tip into the sample at the positive sample bias. The drop in the current at $t = 200$ ms (from 14 to 2.8 pA) was due to the dissociation of CO_2 . (E) Distribution of electron exposure times resulting in dissociation of CO_2 . A total of 500 analyses of the current traces are shown. The sampling bin width was 10 ms. Blue dots represent the numbers of CO_2 dissociation events in the time bins. The data were fitted to a single-exponential decay function with a decay constant $\tau = 0.21$ s. Error bars are $n_t^{1/2}$ (Poisson noise), where n_t is the number of events in time bin t . (F) Log–log plot of the dissociation rate as a function of tunneling current I at a bias voltage of $+2.1$ V. The solid red line is a least-squares fit to the power law I^n . The exponent was found to be $n = 1.03 \pm 0.09$.

Monitoring the tunneling current trace as a function of time during the voltage pulse provides critical information on the electron-induced process.^{10,11} An example of a tunneling current trace during a voltage pulse to a CO_2 feature at $+2.1$ V is shown in Figure 2D. The STM tip was positioned over a selected CO_2 molecule, and a voltage pulse was applied with the tip height maintained at a fixed distance from the CO_2 . The sudden drop in the tunneling current as shown in Figure 2D thus represents a change under the STM tip, in our case corresponding to a successful CO_2 dissociation event. The distribution of the measured electron exposure time (t) resulting in successful CO_2 dissociation events showed an exponential behavior (Figure 2E; see the SI for details). We were able to extract the time constant, τ , which represents the average electron exposure time resulting

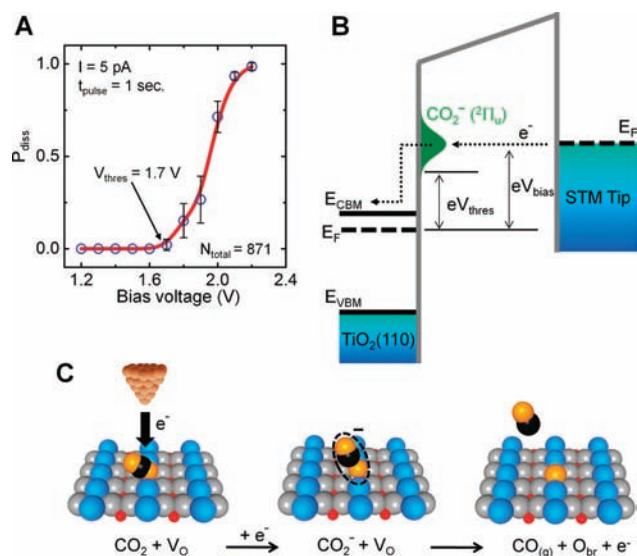


Figure 3. (A) Dissociation probability (P_{diss}) as a function of bias voltage. The threshold voltage was $V_{\text{thres}} = +1.7$ V, and P_{diss} approached 1 at $+2.2$ V. It should be noted that the values of P_{diss} were obtained under a specific voltage pulse condition (5 pA, 1 s). The solid line is a guide to eye. (B) The electron-transfer process at the STM tip/ CO_2 / TiO_2 interface. Above $eV_{\text{thres}} = 1.7$ eV, the electrons start to tunnel into the negative-ion state of the adsorbed CO_2 . (C) Schematics of an electron-induced CO_2 dissociation process. After successful electron transfer from the STM tip, the CO_2 molecule becomes negatively charged (dotted ellipse). The dissociation of CO_2 supplies an oxygen atom that heals the V_{O} site.

in a dissociation event. The dissociation rate (R_{diss}) was then obtained as the reciprocal of the time constant ($1/\tau$). Figure 2F shows a log–log plot of R_{diss} as a function of the tunneling current I for a total of 2262 dissociation events. A least-squares fit of the data yielded a slope $n = 1.03 \pm 0.09$, where n is the exponent in the power-law relationship $R_{\text{diss}} \propto I^n$,¹⁰ indicating that the CO_2 dissociation in our work is a *one-electron-driven* process. The dissociation yield per electron remained nearly constant [$Y_{\text{avg}} = (2.79 \pm 0.63) \times 10^{-7}$] over the current range used in the experiment, as would be expected for a one-electron process (see Figure S3).

The dissociation probability (P_{diss}) was found to depend on the energy of the injected electrons from the STM tip. A plot of P_{diss} as a function of bias voltage at 5 pA (1 s pulse duration) is shown in Figure 3A. We did not observe the dissociation of CO_2 at bias voltages below $+1.6$ V. The threshold voltage (V_{thres}) for the dissociation of CO_2 was $+1.7$ V with a probability $P_{\text{diss}} = 0.02$. The value of P_{diss} increased with increasing bias voltage, eventually approaching 1 at $+2.2$ V. The voltage dependence suggests that the electron-induced dissociation of CO_2 occurs through a well-defined electronic state of CO_2 .

A transient negative ion can be formed in the gas phase upon attachment of a low-energy electron to a molecule, and a metastable negative ion can subsequently dissociate into fragments. This process is called dissociative electron attachment (DEA).²³ It is also known that the lowest-energy DEA process of CO_2 in the gas phase occurs through the $^2\Pi_u$ state.²³ Dissociation of CO_2^- into a neutral CO and an O^- ion occurs after an initial Franck–Condon-type transition of neutral CO_2 to the negative ion followed by internal configuration changes.²³ The weak interaction between CO_2 and the $\text{TiO}_2(110)$ surface suggests

that the electron-induced dissociation of CO_2 adsorbed on $\text{TiO}_2(110)$ occurs through a DEA process similar to that in the gas phase. The main difference for the adsorbed CO_2 is the presence of the V_{O} site on the TiO_2 surface, which can capture the fragment O atom. Because of the large binding energy of O_{br} on TiO_2 ,²⁴ the DEA process for CO_2 adsorbed on $\text{TiO}_2(110)$ may occur more easily than that for CO_2 in the gas phase. The affinity of the V_{O} site for an O atom has also been demonstrated in O_2 dissociation on the $\text{TiO}_2(110)$ surface.²⁵

According to the observed V_{thres} value, tunneling electrons from the Fermi level (E_{F}) of the STM tip can be injected into the CO_2 molecule to form CO_2^- in the $^2\Pi_u$ state *only if* the bias voltage is higher than $V_{\text{thres}} = 1.7$ eV, as shown in Figure 3B. The position of the E_{F} of $\text{TiO}_2(110)$ is ~ 0.3 eV below the CBM of TiO_2 .²⁶ Thus, the threshold energy of CO_2 dissociation is located 1.4 eV above the CBM. In Figure 3C, we schematically illustrate the DEA process for a CO_2 molecule on $\text{TiO}_2(110)$. Specifically, after a tunneling electron from the STM tip is successfully attached to the adsorbed CO_2 molecule, a temporary negative ion (CO_2^-) is formed. Changes in the internal CO_2 configuration such as bending and elongation of the C–O bond occur, as in the gas phase.²³ Upon dissociation of a C–O bond, the O fragment heals the V_{O} site and is incorporated into the O_{br} row. The CO fragment desorbs from the surface or moves away from the reaction site, probably because it is in an excited state with some excess energy gained during the dissociation process. The excess electron most likely dissipates into the conduction band of $\text{TiO}_2(110)$.

In summary, we have demonstrated the electron-induced dissociation of CO_2 on $\text{TiO}_2(110)$ at the atomic scale by using STM in an attempt to mimic the initial step of CO_2 activation on a photocatalyst surface. Our results highlight the importance of the relative energy level of CO_2 with respect to the CBM of TiO_2 in the photocatalytic reduction process. In a TiO_2 photocatalyst sensitized with chromophores such as quantum dots, the photoexcited electrons in the photosensitizer are initially transferred to the conduction band of TiO_2 .²⁷ The electrons quickly relax to the bottom of the conduction band through electron–phonon scattering.⁴ However, our value of the threshold energy for CO_2 dissociation indicates that the electron affinity level of CO_2 lies at least 1.4 eV above the CBM of TiO_2 . This sets the minimum energy of the electron above the CBM required to activate CO_2 under “dry” vacuum conditions. The efficiency of the initial CO_2 activation step (i.e., charging by the photogenerated electron) is significantly reduced as a result of electron relaxation within the conduction band. The results point to the need for a solvent- or coadsorbate-aided CO_2 activation process for more efficient photocatalytic reduction of CO_2 .

■ ASSOCIATED CONTENT

S Supporting Information. Experimental procedures, theoretical methods, and supporting figures. This material is available free of charge via the Internet at <http://pubs.acs.org>.

■ AUTHOR INFORMATION

Corresponding Author
junseok.lee@netl.doe.gov

■ ACKNOWLEDGMENT

The research was performed in support of the National Energy Technology Laboratory’s ongoing research under RES Contract

DE-FE0004000. J.L. and D.C.S. thank A. Cugini for support and helpful discussions. J.L. thanks C. Wang for helpful discussions during the preparation of the manuscript.

REFERENCES

- (1) Lewis, N. S.; Nocera, D. G. *Proc. Natl. Acad. Sci. U.S.A.* **2006**, *103*, 15729.
- (2) Chueh, W. C.; Falter, C.; Abbott, M.; Scipio, D.; Furler, P.; Haile, S. M.; Steinfeld, A. *Science* **2010**, *330*, 1797.
- (3) Morris, A. J.; Meyer, G. J.; Fujita, E. *Acc. Chem. Res.* **2009**, *42*, 1983.
- (4) Prezhdo, O. V.; Duncan, W. R.; Prezhdo, V. V. *Prog. Surf. Sci.* **2009**, *84*, 30.
- (5) Fujishima, A.; Honda, K. *Nature* **1972**, *238*, 37.
- (6) Inoue, T.; Fujishima, A.; Konishi, S.; Honda, K. *Nature* **1979**, *277*, 637.
- (7) Diebold, U. *Surf. Sci. Rep.* **2003**, *48*, 53.
- (8) Centi, G.; Perathoner, S. *Catal. Today* **2009**, *148*, 191.
- (9) Linsebigler, A. L.; Lu, G. Q.; Yates, J. T., Jr. *Chem. Rev.* **1995**, *95*, 735.
- (10) Stipe, B. C.; Rezaei, M. A.; Ho, W.; Gao, S.; Persson, M.; Lundqvist, B. I. *Phys. Rev. Lett.* **1997**, *78*, 4410.
- (11) Pascual, J. I.; Lorente, N.; Song, Z.; Conrad, H.; Rust, H. P. *Nature* **2003**, *423*, 525.
- (12) Komeda, T.; Kim, Y.; Fujita, Y.; Sainoo, Y.; Kawai, M. *J. Chem. Phys.* **2004**, *120*, 5347.
- (13) Sloan, P. A.; Palmer, R. E. *Nature* **2005**, *434*, 367.
- (14) Diebold, U.; Anderson, J. F.; Ng, K. O.; Vanderbilt, D. *Phys. Rev. Lett.* **1996**, *77*, 1322.
- (15) Suzuki, S.; Fukui, K.; Onishi, H.; Iwasawa, Y. *Phys. Rev. Lett.* **2000**, *84*, 2156.
- (16) Sorescu, D. C.; Lee, J.; Al-Saidi, W. A.; Jordan, K. D. *J. Chem. Phys.* **2011**, *134*, No. 104707.
- (17) Henderson, M. A. *Surf. Sci.* **1998**, *400*, 203.
- (18) Thompson, T. L.; Diwald, O.; Yates, J. T., Jr. *J. Phys. Chem. B* **2003**, *107*, 11700.
- (19) Maksymovych, P.; Sorescu, D. C.; Dougherty, D.; Yates, J. T., Jr. *J. Phys. Chem. B* **2005**, *109*, 22463.
- (20) Lee, J.; Zhang, Z.; Deng, X.; Sorescu, D. C.; Matranga, C.; Yates, J. T., Jr. *J. Phys. Chem. C* **2011**, *115*, 4163.
- (21) Calvaresi, M.; Martinez, R. V.; Losilla, N. S.; Martinez, J.; Garcia, R.; Zerbetto, F. *J. Phys. Chem. Lett.* **2010**, *1*, 3256.
- (22) Huber, K. P.; Herzberg, G. *Constants of Diatomic Molecules; Molecular Spectra and Molecular Structure*, Vol. 4; Van Nostrand Reinhold: New York, 1979.
- (23) Christophorou, L. G.; McCorkle, D. L.; Christodoulides, A. A. In *Electron-Molecular Interactions and Their Applications*; Christophorou, L. G., Ed.; Academic Press: New York, 1983; Vol. 1.
- (24) Ganduglia-Pirovano, M. V.; Hofmann, A.; Sauer, J. *Surf. Sci. Rep.* **2007**, *62*, 219.
- (25) Scheiber, P.; Riss, A.; Schmid, M.; Varga, P.; Diebold, U. *Phys. Rev. Lett.* **2010**, *105*, No. 216101.
- (26) Tisdale, W. A.; Williams, K. J.; Timp, B. A.; Norris, D. J.; Aydil, E. S.; Zhu, X.-Y. *Science* **2010**, *328*, 1543.
- (27) Watson, D. F.; Meyer, G. J. *Annu. Rev. Phys. Chem.* **2005**, *56*, 119.